Geophysical Research Letters

RESEARCH LETTER
10.1029/2020GL091418

Special Section:
The Arctic: An AGU Joint Special Collection

Supraglacial River Forcing of Subglacial Water Storage and Diurnal Ice Sheet Motion

L. C. Smith[1,2,3], L. C. Andrews[4], L. H Pitcher[5,3], B. T. Overstreet[6], Å. K. Rennermalm[7], M. G. Cooper[3,8], S. W. Cooley[9,3], J. C. Ryan[1], C. Miège[7,10], C. Kershner[11,13], and C.E. Simpson[12,3]

[1]Institute at Brown for Environment and Society, Brown University, Providence, RI, USA, [2]Department of Earth, Environmental, and Planetary Sciences, Brown University, Providence, RI, USA, [3]Department of Geography, University of California-Los Angeles, Los Angeles, CA, USA, [4]Global Modeling and Assimilation Office, NASA Goddard Space Flight Center, Greenbelt, MD, USA, [5]Cooperative Institute for Research in Environmental Sciences, University of Colorado-Boulder, Boulder, CO, USA, [6]Department of Geology and Geophysics, University of Wyoming, Laramie, WY, USA, [7]Department of Geography, Rutgers, State University of New Jersey, New Brunswick, NJ, USA, [8]Atmospheric Sciences and Global Change Division, Pacific Northwest National Laboratory, Richland, WA, USA, [9]Department of Earth System Science, Stanford University, Stanford, CA, USA, [10]Department of Geography, University of Utah, Salt Lake City, UT, USA, [11]Research Directorate, National Geospatial-Intelligence Agency, Springfield, VA, USA, [12]RedCastle Resources Inc., Salt Lake City, UT, USA, [13]Department of Geography and Geoinformation Science, George Mason University, Fairfax, VA, USA

Key Points:

- We measure supraglacial river discharge entering a major moulin simultaneously with local accelerations in ice sheet motion
- Recorded ice speeds are strongly correlated with diurnal cycles of moulin input over the 168 hour field experiment
- Differencing supraglacial and proglacial hydrographs suggests diurnal fluctuations in subglacial water storage drive short-term ice motion

Supporting Information:

Supporting Information may be found in the online version of this article.

Correspondence to:

L. C. Smith,
laurence_smith@brown.edu

Citation:

Smith, L. C., Andrews, L. C., Pitcher, L. H., Overstreet, B. T., Rennermalm, Å. K., Cooper, M. G., et al. (2021). Supraglacial river forcing of subglacial water storage and diurnal ice sheet motion. *Geophysical Research Letters*, *48*, e2020GL091418. https://doi.org/10.1029/2020GL091418

Received 16 NOV 2020
Accepted 15 FEB 2021

Abstract Surface melting impacts ice sheet sliding by supplying water to the bed, but subglacial processes driving ice accelerations are complex. We examine linkages between surface runoff, transient subglacial water storage, and short-term ice motion from 168 consecutive hourly measurements of meltwater discharge (moulin input) and GPS-derived ice surface motion for Rio Behar, a ~60 km^2 moulin-terminating supraglacial river catchment on the southwest Greenland Ice Sheet. Short-term accelerations in ice speed correlate strongly with lag-corrected measures of supraglacial river discharge ($r = 0.9$, $\tau = 0.7$, $p < 0.01$). Though our 7 days record cannot address seasonal-scale forcing, diurnal ice accelerations align with normalized differenced supraglacial and proglacial discharge, a proxy for subglacial storage change, better than GPS-derived ice surface uplift. These observations counter theoretical steady state basal sliding laws and suggest that moulin and proglacially induced fluctuations in subglacial water storage, rather than absolute subglacial water storage, drive short-term ice accelerations.

Plain Language Summary The importance of surface meltwater runoff to Greenland ice sheet subglacial hydrology and ice sliding dynamics is widely recognized but poorly constrained by field observations. We present 168 consecutive hours of rare in situ discharge measurements in a large supraglacial river draining the ice sheet surface, just upstream of where it plummets into a major moulin. GPS measurements of ice surface motion record brief accelerations in ice sliding speed that follow daily cycles in meltwater entering the moulin. By comparing these measurements with proglacial river discharges leaving the ice sheet, we identify daily fluctuations in subglacial water storage that track short-term accelerations in ice motion. These findings affirm the importance of supraglacial rivers to subglacial water pressure and ice dynamics, even in relatively thick ice >40 km inland from the ice terminus.

1. Introduction

Accurate models of ice sheet response to climate change require good physical understanding of interactions between surface melting, subglacial hydrology, and ice dynamics (e.g., Bell, 2008; Chu, 2014; Davison et al., 2019). On the Greenland Ice Sheet (GrIS) ablation zone, surface melting activates a perennial hydrologic system of supraglacial streams, rivers, and lakes (Irvine-Fynn et al., 2011; Lampkin & VanderBerg, 2014; Pitcher & Smith, 2019; Rennermalm et al., 2013), which commonly drain into moulins forming a dynamic subglacial drainage system that modifies basal pressures and ice motion (e.g., Bartholomew et al., 2012; Meierbachtol et al., 2013; Van de Wal et al., ; Zwally et al., 2002). While early concerns about warming-induced runaway sliding now seem unfounded (e.g., Flowers, 2018; Tedstone et al., 2015, 2013; van de Wal et al., 2015), physical processes linking GrIS supraglacial meltwater runoff, ice sheet basal pressures, and ice sliding remain under intense study (Davison et al., 2019; Nienow et al., 2017; Williams

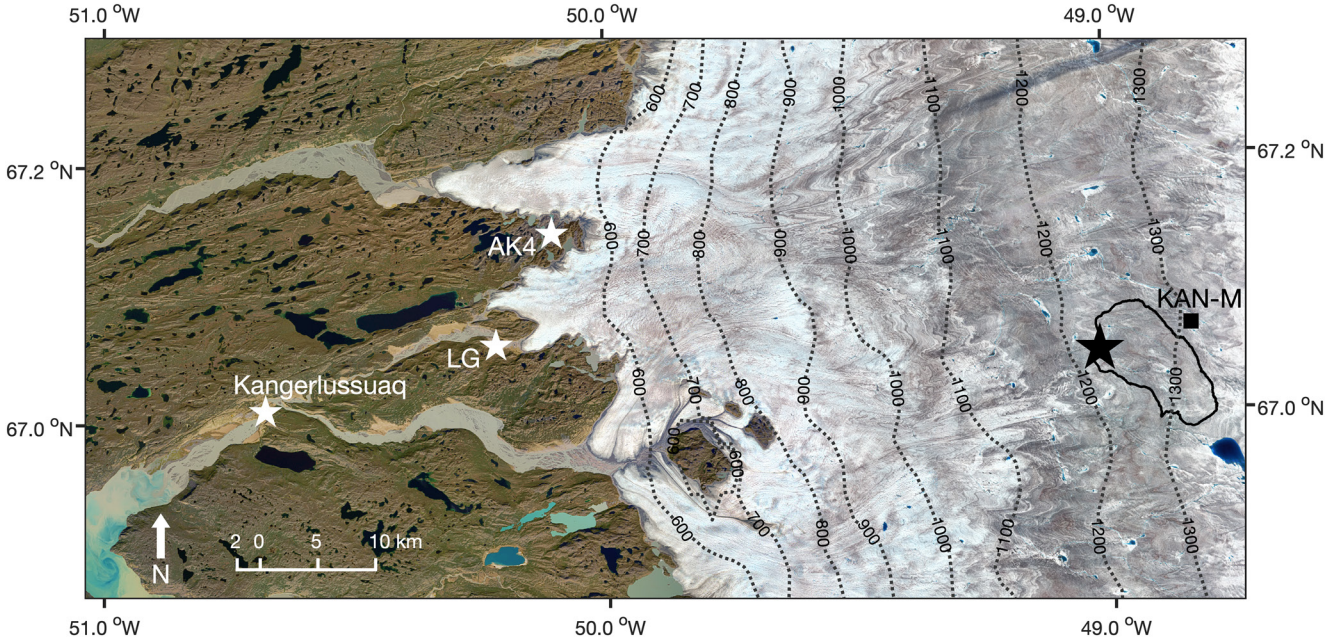

Figure 1. Study area in southwest Greenland. Black star shows location of our GPS measurements of ice surface motion and Acoustic Doppler Current Profiler (ADCP) measurements of moulin input (supraglacial discharge) in Rio Behar, a large supraglacial river penetrating the ice sheet >40 km from the ice edge. Field work was conducted ~750 m upstream of the Rio Behar terminal moulin. Black outline delineates the surface catchment (60.02 km^2 in July 2016). White stars locate proglacial river gauging stations; black square locates PROMICE KAN_M automated weather station. Background is a July 26, 2016 true-color Landsat-8 satellite image.

et al., 2020), particularly processes governing englacial connectivity and subglacial evolution due to surface melting (e.g., Christoffersen et al., 2018; Poinar et al., 2015; Stevens et al., 2015).

Traditional basal sliding law formulations linking subglacial pressure and ice motion assume steady state basal cavities (e.g., Bindschadler, 1983; Gagliardini et al., 2007; Schoof, 2005). However, observational research suggests that cavities constantly undergo transient evolution in response to fluctuations in supraglacial meltwater supply and subglacial channelization (Andrews et al., 2018; Bartholomaus et al., 2008; Cowton et al., 2016; Hoffman et al., 2011; Iken et al., 1983). If so, highest subglacial water pressures (and therefore ice sliding speeds) should occur when transient cavities are growing fastest, not when they are largest (Cowton et al., 2016; Iken et al., 1983).

Evidence for transient cavity evolution is drawn primarily from GPS-derived correlations of horizontal ice speed with vertical ice surface uplift (interpreted as a proxy for total subglacial water storage, S) or its first derivative (interpreted as subglacial water storage rate-of-change, ΔS). GrIS horizontal ice sliding speed broadly covaries with vertical surface uplift over seasonal time scales (e.g., Bartholomew et al., 2012, 2010; Hoffman et al., 2011), but variations at shorter timescales tend to correlate better with its derivative (Andrews et al., 2018; Cowton et al., 2016; Hoffman et al., 2011). Such correlations are typically weak and spatially variable due to a range of factors confounding estimation of basal uplift from ice surface elevation measurements (Andrews et al., 2018; Hoffman et al., 2011). Therefore, it is difficult to infer interactions between surface melting, subglacial water storage, cavity growth, and ice motion for the GrIS, despite previous success on mountain glaciers (e.g., Armstrong & Anderson, 2020; Bartholomaus et al., 2011, 2008)

To study the links among supraglacial runoff, subglacial water storage fluctuations, and short-term ice motion, we present in situ measurements of moulin input (i.e., supraglacial discharge), ice surface speed, and ice surface uplift for Rio Behar, a large supraglacial river on the GrIS midelevation (>1,200 m a.s.l.) ablation zone (Figure 1). We compare daily cycles in these variables with PROMICE automated weather station (AWS) measurements of surface energy balance and ablation (Fausto & van As, 2019), and with proglacial river discharges from three gauging stations downstream (Rennermalm et al., 2017; Tedstone et al., 2017; van As et al., 2019). We present GPS measurements of horizontal ice surface speed and vertical uplift,

and use them to estimate subglacial storage S and rate-of-change ΔS, respectively. We also compute alternate proxies for S and ΔS by differencing normalized supraglacial and proglacial discharge hydrographs (adapted from Bartholomaus et al., 2008, 2011; McGrath et al., 2011; Armstrong & Anderson, 2020). We conclude that diurnal cycles in supraglacial river discharge drive ice accelerations through ΔS, confirming that transient water storage and cavity growth are important influences on GrIS subglacial basal pressure and short-term ice motion.

2. Data and Methods

2.1. Observational Data

In July 2016, the Rio Behar terminal moulin was located at 67.047°N, −49.033°W, with an upstream drainage catchment of ~60.2 km^2 and mean surface elevation >1,200 m (Figure 1). We established a field camp to measure moulin meltwater input and ice surface motion ~750 m upstream (~67.050°N, −49.018°W). During July 5–13, 2016, we collected 174 measurements of supraglacial river discharge using a SonTek RiverSurveyor M9 Acoustic Doppler Current Profiler (ADCP) and methods of Smith et al. (2017). A Tyrolean cableway was suspended over the river to safely and repeatedly tow the ADCP back and forth across the channel every hour (Figures S1–S4). In total 847 ADCP transects were acquired, of which 677 later passed rigorous quality-assurance screening and were used to compute 168 consecutive hourly discharge measurements from July 6–13 (Text S1–S3, Figure S5, Tables S1–S2, and Data sets S1–S2).

Simultaneous measurements of ice surface motion were collected every 5-s using a Trimble R7 GPS receiver and Trimble Zephyr Geodetic antenna anchored 3m into the ice to prevent its movement from ablation (67.048°N, −49.018°W, elevation 1211.43 m). On-ice kinematic GPS positions were later estimated using carrier-phase differential processing relative to a bedrock mounted base station (~47 km baseline, 67.150°N, −50.058°W, elevation 581.19) and final International GNSS Service satellite orbits (Andrews et al., 2014, 2018; Chen, 1998; Estey & Meertens, 1999; Hoffman et al., 2011; Text S4). To assess surface melt processes, simultaneous measurements of 2-m air temperature, energy balance, and ablation were obtained from the nearby PROMICE KAN_M AWS (Fausto & van As, 2019, Text S5). Proglacial river discharges were obtained from gauges at Qinnguata Kuussua/Watson River in Kangerlussuaq (van As et al., 2019), its northern tributary Akuliarusiarsuup Kuua (AK4) near the ice terminus (Rennermalm et al., 2017, AK4 station), and a discontinued gauge near Leverett Glacier (Tedstone et al., 2017) (Figure 1). Lagged correlation coefficients (e.g., Armstrong & Anderson, 2020; Flowers et al., 2016) were used to quantify links between these variables and GPS-derived ice motion, and to compute proglacial timing delays between the ice edge and Kangerlussuaq (Texts S6, S8).

2.2. Proxies for S and ΔS

GPS-derived vertical positions and their first derivative were used to estimate subglacial storage S and rate-of-change ΔS (e.g., Bartholomew et al., 2012; Cowton et al., 2016; Text S7). Proxies for S and ΔS were also computed by adapting a meltwater input-output approach (Armstrong & Anderson, 2020; Bartholomaus et al., 2008, 2011; McGrath et al., 2011) comparing relative timings of supraglacial and proglacial river discharge hydrographs (Text S7). Hydrographs were normalized and differenced (supraglacial minus proglacial) to assess their relative timings and shapes at Rio Behar moulin versus at the ice edge. These "discharge-difference" proxies are unitless and do not satisfy mass conservation. They characterize instantaneous net water storage changes, not subglacial routing delays and/or storages known to retard proglacial discharges longer than 24 h (e.g., Chandler et al., 2013; Chu et al., 2016; Pitcher et al., 2020; Rennermalm, Smith, et al., 2013; Smith et al., 2015; van As et al., 2017). From dye tracing experiments, subglacial routing from ~1,300 m elevation takes 1–3 days (Chandler et al., 2013, site L57), or ~2–5 days from proglacial hydrograph analysis (van As et al., 2017). Such subglacial delays and storages are irrelevant to our purpose here, which is simply to characterize instantaneous subglacial conditions at our field site, not Lagrangian transport to the ice edge. Descriptions of all data, methods, and uncertainties are presented in SI (Texts S1–S9, Figures S7–S14, Tables S1–S5).

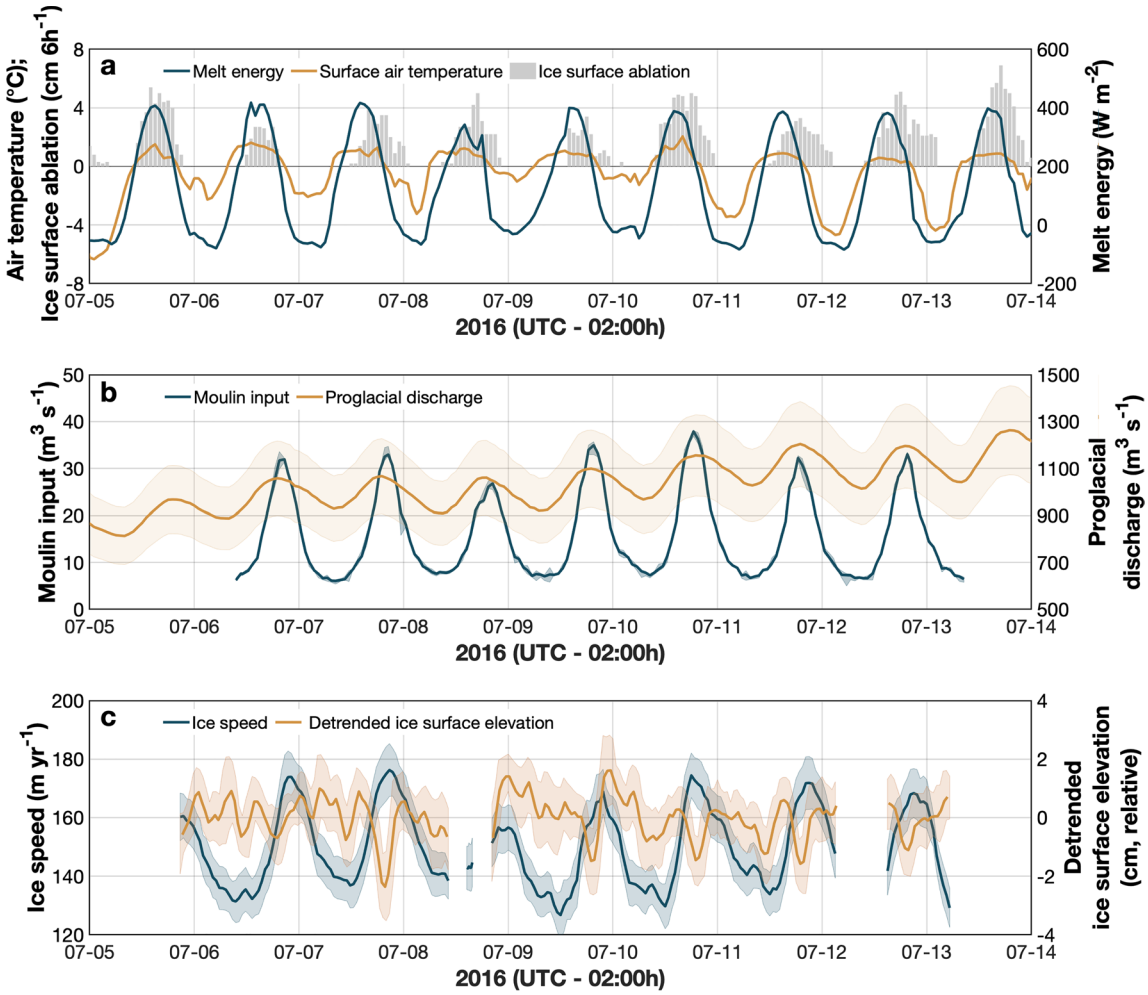

Figure 2. In situ measurements of (a) melt energy, air temperature, and ice ablation from KAN_M; (b) Rio Behar moulin input (supraglacial discharge) and proglacial discharge measured at Kangerlussuaq (-5h timing correction applied); (c) ice surface speed and elevation. Colored envelopes (b), (c) represent measurement uncertainties.

3. Results

3.1. Correlations of Ice Speed with Other Variables

We find strong diurnal cycles in all variables except surface elevation, with daily accelerations in horizontal ice speed closely tracking moulin input and melt energy (Figure 2 and Table S3). A consistent progression is observed in the timing of daily peaks, with melt energy and air temperatures peaking near local solar noon, followed by sequential peaks in ice ablation, proglacial discharge, moulin input, and horizontal ice speed (Figure 3). The timing of daily peaks is most consistent for melt energy, proglacial discharge, moulin input, and ice speed, whereas peaks in air temperature, ablation, and especially ice surface elevation are more variable as indicated by their peak timing range (Table S3).

After lagging our GPS-derived horizontal ice speed time-series to correct for its mean timing offsets with the other variables, we compute correlations between potential forcing variables and ice speed using Pearson's r, which assumes a linear relationship, and Mann-Kendall's τ, which does not assume a linear relationship between variables. We find that ice speed correlates strongly with moulin input ($r = 0.90$, $\tau = 0.70$), melt energy ($r = 0.90$, $\tau = 0.67$), and proglacial discharge ($r = 0.88$, $\tau = 0.71$) (Figure 4 and Table S4). We find moderately strong correlations with ice surface ablation ($r = 0.74$, $\tau = 0.59$) and air temperature ($r = 0.70$, $\tau = 0.54$), which are drivers of runoff and melt energy, respectively. Lowest correlation is found for

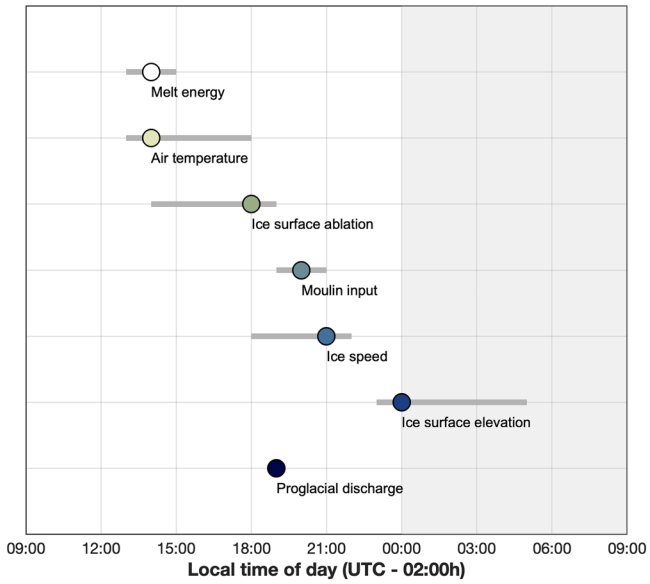

Figure 3. Mean daily peak timing (circles) and timing range (gray bars) of observed variables. Diurnal cycles in melt energy and air temperatures peak around solar noon, followed by peaks in ice ablation, proglacial discharge, moulin input, ice speed, and ice surface uplift. GPS-derived daily peaks in uplift are temporally variable (Table S3). Peak proglacial discharge has little timing variability and is shifted −5 h earlier to account for the mean timing offset between Kangerlussuaq and the ice edge. This figure presents only timing of daily peaks, not subglacial routing delays and/or storages of meltwater.

detrended ice surface elevation (i.e., uplift, $r = 0.36$, $\tau = 0.24$, Table S4 and Figure 4e). All correlations are statistically significant ($p < 0.01$). Unlike melt energy (which turns negative, implying nocturnal refreezing), moulin input persists throughout the night. Because (i) moulin input closely tracks (and derives from) melt energy; (ii) virtually all surface runoff generated within Rio Behar catchment flows to its terminal moulin; and (iii) an observed 6h time lag between peak melt energy and peak supraglacial discharge (Table S3) is similar to a previously calculated catchment routing delay for Rio Behar (i.e., estimated time-to-peak $t_p = 5.5$ h, Smith et al., 2017) we infer that supraglacial river discharge, a product of catchment-integrated melt energy, is the dominant supraglacial forcing variable driving our locally recorded ice speed variations.

3.2. Comparison of Short-Term Ice Accelerations with S and ΔS

To further investigate drivers of short-term ice speed variations, we test proxies of subglacial water storage S and rate-of-change ΔS calculated from GPS-derived ice surface observations (following Anderson et al., 2004; Andrews et al., 2018; Cowton et al., 2016; Harper et al., 2007; Hoffman et al., 2011; Howat et al., 2008) and by differencing normalized hydrographs of supraglacial and proglacial river discharge (Texts S7–S9). Implicit in the latter "discharge-difference" calculations are assumptions that englacial storage is negligible; that en/subglacial melting is negligible; that subglacial routing delays are irrelevant to instantaneous net storage; and that proglacial discharge reflects overall regional basal water pressure, allowing Rio Behar moulin input to be compared with regional proglacial discharge despite its smaller spatial domain (60 km^2 versus ~2,800 km^2 to 1,750 m a.s.l.) and absolute discharge magnitude (~6–38 m s^{-1} versus ~800–1,300 m^3 s^{-1}).

Comparison of our observed horizontal ice speeds with both proxies for S and ΔS suggests that ΔS drives short-term accelerations in ice speed (Figures 5, S11, S13, S14 and Table S5). This conclusion is clearest from the discharge-difference proxies, with ΔS tracking ice as well or better than S (see Figure 5c versus 5b; S13c versus S13b; Figures S11d, S14d vs. S11c, S14c). This same conclusion may be drawn, albeit less compellingly, from conventional GPS-derived S and ΔS proxies (Figure 5a versus Figure 2c; Figures S11b, S14b versus S11a, S14a). For both methods, ΔS generally correlates with ice accelerations better than S (Table S5) suggesting that changes in subglacial water storage force short-term ice speed accelerations at our field site.

4. Discussion and Conclusion

We find that diurnal cycles in moulin input are the primary driver of short-term accelerations in ice sliding velocity at our field site (Figure 4). This finding supports previous work (Andrews et al., 2014) and the conclusion that over short time scales, diurnal variability in supraglacial river input imposes a first-order control on subglacial water pressure fluctuations. Furthermore, while short-term accelerations in ice speed closely follow moulin input, they also tend to track proxies of subglacial water storage change (ΔS) better than proxies of absolute storage (S) (Figures 5, S11, S13, and S14), suggesting that nightly peaks in subglacial water storage drive subglacial basal pressure and short-term ice motion.

This conclusion is more evident in discharge-difference proxies than conventional GPS-derived proxies (e.g., Figures 5c versus 5a; S13c versus S13a; S11d, S14d versus S11b, S14b). This is likely due to our inability to assess the impact of changes in the ice column due to variations in vertical strain, making our GPS-derived proxies susceptible to local and nonlocal forcings (e.g., Price et al., 2008; Ryser et al., 2014; see Text S7). Differencing supraglacial and proglacial hydrographs, therefore, may characterize subglacial water storage conditions more sensitively than small vertical ice surface elevation changes, which are inherently difficult to detect and have multiple sources of uncertainty (Anderson et al., 2004; Andrews et al., 2018).

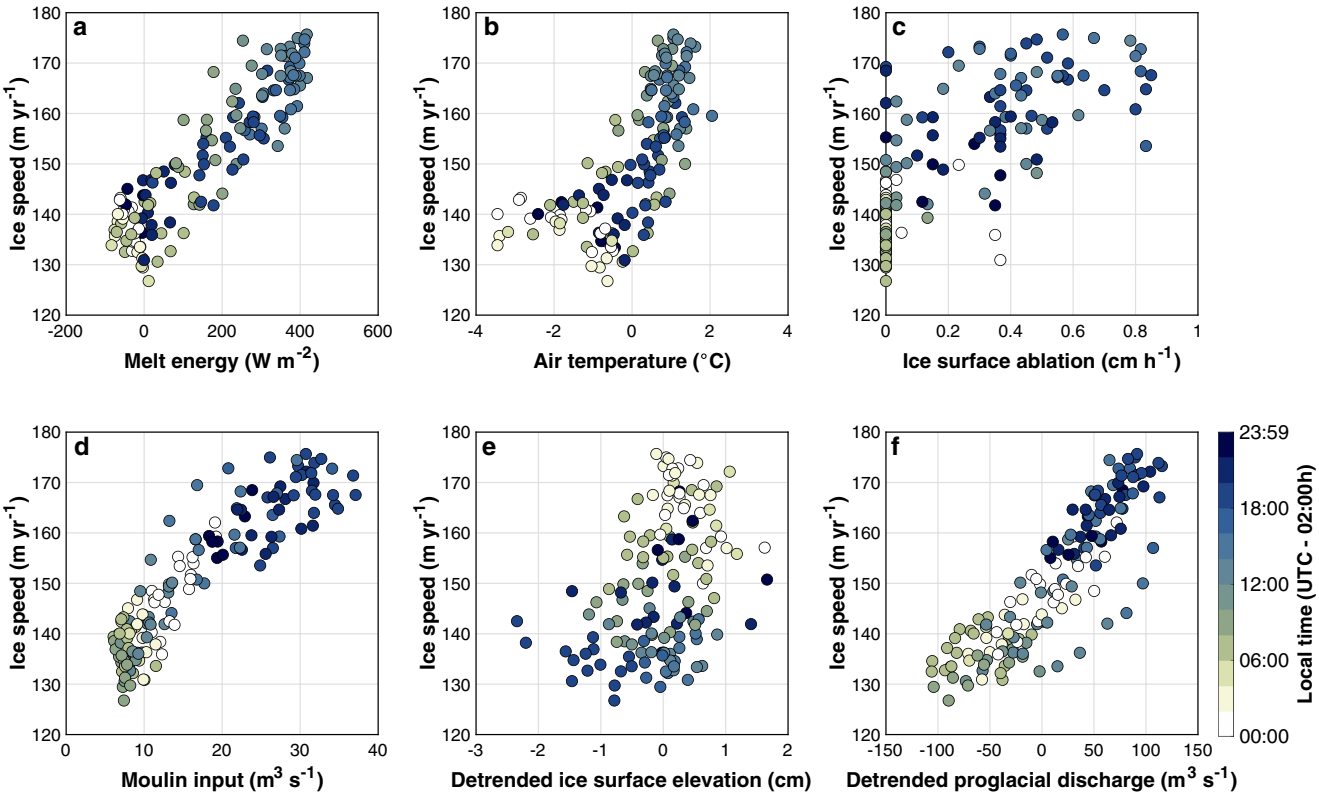

Figure 4. Correlations between ice speed and other variables, after correcting for their mean differences (values in parentheses) in daily peak timing: (a) melt energy (−7 h); (b) air temperature (−8 h); (c) ablation (−4 h); (d) moulin input (−2 h); (e) ice surface elevation (+6 h); (f) proglacial discharge (−2 h at terminus). Statistical correlations presented in Table S4. Moulin input displays strongest correlation with ice speed ($r = 0.90$, $\tau = 0.70$, $p < 0.01$).

A discharge input-output approach (e.g., Armstrong & Anderson, 2020; Bartholomaus et al., 2011, 2008; McGrath et al., 2011), comparing moulin inputs with proglacial outputs, offers an alternate strategy for characterizing subglacial water storage and its link to basal sliding laws. Future studies, for example, could develop discharge-difference proxies over longer time scales and larger study areas by pairing surface-routed climate model output (e.g., Smith et al., 2017; Yang et al., 2019) with proglacial discharge records (Rennermalm et al., 2017; van As et al., 2019), to relate net increases/decreases in ΔS to regional ice speed variations.

It is well-known that evolution of the subglacial system from inefficient to efficient states acts to modulate the ice dynamical response to supraglacial water inputs (e.g., Bartholomew et al., 2010; 2011; Hoffman et al., 2011). We find that peak or ascendant ΔS is associated with localized GrIS velocity accelerations (Figures 5c and S13c). This suggests that highest subglacial water pressure (and ice sliding speed) occurs when subglacial cavities are growing the fastest, not when their volume is largest (e.g., Cowton et al., 2016; Iken et al., 1983). As such, steady state theoretical basal sliding laws—which assume a relationship between cavity size and subglacial pressure – do not accurately represent transient behavior of the subglacial system.

It is important to note that the strong correlation between moulin input and ice velocity reported here (Figure 4d) is unlikely to hold over an entire melt season. Previous work has clearly established that Greenland ice sliding velocities are strongly influenced by long-term seasonal evolution of the subglacial hydrological system (e.g., Andrews et al., 2018; Bartholomew et al., 2010; Hoffman et al., 2011; Nienow et al., 2017). Our short 7 days record captures neither the early nor late melt season, when subglacial efficiency (and associated ice speeds) undergo extensive changes. Subglacial evolution makes melt-driven proxies inappropriate for estimating ice motion over the entire melt season (Andrews et al., 2014; Bartholomew et al., 2010) or multiple years (Davison et al., 2019; Tedstone et al., 2015). Over short time scales, however, we find that diurnal cycles in moulin input are the primary driver of fluctuating subglacial water pressures and associated ice accelerations—even in relatively thick ice (~1 km) more than 40 km inland from the ice edge. Some slight

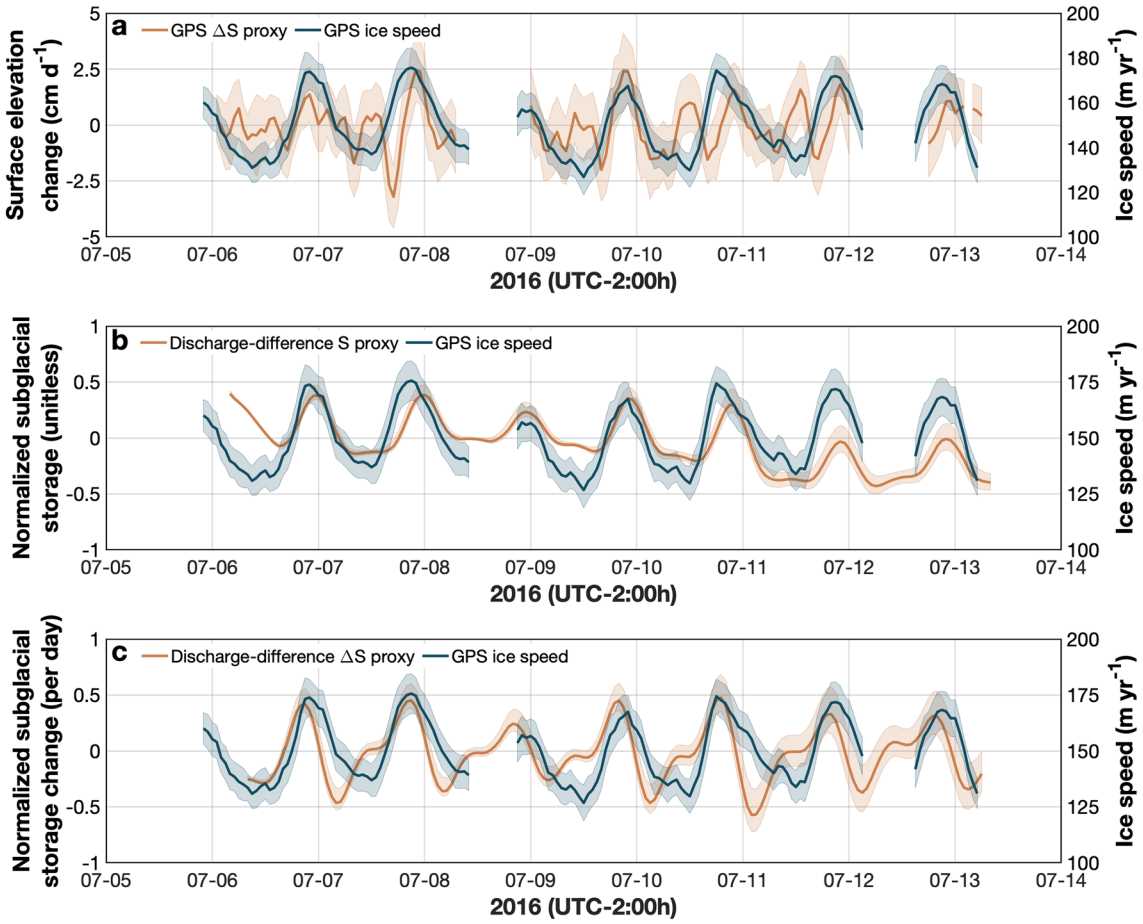

Figure 5. Comparison of horizontal ice speed (blue) with proxies for subglacial water storage (S) and storage rate-of-change (ΔS): (a) ΔS estimated from GPS-derived ice surface elevation; (b) S estimated from normalized discharge-difference; (c) ΔS estimated from normalized discharge-difference. See Figure 2c for S estimated from GPS. Brief accelerations in ice speed track ΔS (c) better than S (b), and discharge-difference (c) tracks ice speed better than GPS (a). Figure S13 presents another version of this figure using AK4 proglacial discharges.

differences in peak timings between ΔS and ice motion, as well as some nonlinear behavior on descending limbs (Figures 5c and 13c) are discussed further in Text S9.

This study adds to a small but growing collection of GrIS supraglacial streamflow measurements (Carver et al., 1994; Chandler et al., 2013; Echelmeyer & Harrison, 1990; Gleason et al., 2016; Holmes, 1955; McGrath et al., 2011; Smith et al., 2015, 2017). With peak daily discharges of 26.59–37.61 m^3/s (Table S2), the discharges reported here are far larger than those collected in most supraglacial streams, but are typical for trunk supraglacial rivers in southwest Greenland (Smith et al., 2015, 2017). Nearly all of them terminate in moulins (Smith et al., 2015; Yang & Smith, 2016), and the high diurnal variability we observe (ranging from 19.05 to 30.50 m^3/s, Table S2) signifies that their subglacial channels are likely out of equilibrium with supraglacial inputs for large portions of the day, such that associated accelerations in ice speed are driven by addition or removal of water outside of the channelized system.

Based on satellite mapping (e.g., Lampkin & VanderBerg, 2014; Smith et al., 2015; Yang et al., 2015, 2016; Yang & Smith, 2013, 2016) and topographic modeling (e.g., Banwell et al., 2016, 2012; Crozier et al., 2018; Karlstrom & Yang, 2016; King et al., 2016), we maintain that supraglacial rivers likely drive ice accelerations near hundreds of other terminal moulins as well. Process-level understanding and modeling of subglacial hydrology and associated ice dynamics should presume large, strongly diurnal inputs of meltwater entering hundreds of supraglacial river moulins distributed throughout Greenland's ablation zone. These inputs, countered by water output discharged beneath outlet glaciers, trigger short-term fluctuations in subglacial water storage that drive short-term accelerations in ice sheet motion.

Data Availability Statement

Discharge data, surface mass balance data, ADCP and GPS data summaries, S and ΔS proxies, and a time-lapse camera video are available as tables (Tables S1–S2) and/or Additional Supporting Information (Data set S1–S9). Original, full-resolution ADCP and GPS data are archived at the Arctic Data Center (https://doi.org/10.18739/A22F7JS1B). PROMICE KAN_M automated weather station data (Fausto & van As, 2019) are available from https://www.promice.org/PromiceDataPortal/. Proglacial river discharges for Qinnguata Kuussua/Watson River (van As et al., 2019), Akuliarusiarsuup Kuua (Rennermalm et al., 2013b, 2017), and Leverett Glacier (Tedstone et al., 2017) are available from https://doi.org/10.22008/promice/data/watson_river_discharge, https://doi.org/10.1594/PANGAEA.876357, and https://doi.org/10.5285/17c400f1-ed6d-4d5a-a51f-aad9ee61ce3d. Original GPS data files are also archived at UNVACO (https://www.unavco.org/data/doi/10.7283/GT6K-B184).

Acknowledgments
We dedicate this paper to the memory of Dr. Konrad Steffen (1952–2020). This research was funded by the NASA Cryospheric Science Program (Grants 80NSSC19K0942 and NNX14AH93G) managed by Dr. Thorsten Markus. Polar Field Services, Inc. and Kangerlussuaq International Science Support (KISS) provided logistical field support. GPS equipment was loaned by UNAVCO, Inc. with support from NASA and NSF. A. Zaino and J. Pettit of UNAVCO advised on GPS receiver hardware, programming, and installation. Proglacial discharge data from Qinnguata Kuussua/Watson River were gathered by the University of Copenhagen and the Geological Survey of Denmark and Greenland. The KAN_M weather station is part of the Program for Monitoring of the Greenland Ice Sheet (www.PROMICE.dk). We thank Mathieu Morlighem, William Armstrong and an anonymous reviewer for deeply constructive reviews. The authors declare there are no real or perceived financial conflicts of interest, or other affiliations for any author that may be perceived as having a conflict of interest with respect to the results of this research.

References

Anderson, R. S., Anderson, S. P., MacGregor, K. R., Waddington, E. D., O'Neel, S., Riihimaki, C. A., & Loso, M. G. (2004). Strong feedbacks between hydrology and sliding of a small alpine glacier. *Journal of Geophysical Research*, *109*, F03005. https://doi.org/10.1029/2004JF000120

Andrews, L. C., Catania, G. A., Hoffman, M. J., Gulley, J. D., Lüthi, M. P., et al. (2014). Direct observations of evolving subglacial drainage beneath the Greenland Ice Sheet. *Nature*, *514*, 80–83. https://doi.org/10.1038/nature13796

Andrews, L. C., Hoffman, M. J., Neumann, T. A., Catania, G. A., Lüthi, M. P., Hawley, R. L., et al. (2018). Seasonal evolution of the subglacial hydrologic system modified by supraglacial lake drainage in western Greenland. *Journal of Geophysical Research: Earth Surface*, *123*, 1479–1496. https://doi.org/10.1029/2017JF004585

Armstrong, W. H., & Anderson, R. S. (2020). Ice-marginal lake hydrology and the seasonal dynamical evolution of Kennicott Glacier, Alaska. *Journal of Glaciology*, *66*(259), 699–713. https://doi.org/10.1017/jog.2020.41

Banwell, A. F., Arnold, N. S., Willis, I. C., Tedesco, M., & Ahlstrom, A. P. (2012). Modeling supraglacial water routing and lake filling on the Greenland ice sheet. *Journal of Geophysical Research*, *117*, F04012. https://doi.org/10.1029/2012JF002393

Banwell, A., Hewitt, I., Willis, I., & Arnold, N. (2016). Moulin density controls drainage development beneath the Greenland ice sheet. *Journal of Geophysical Research: Earth Surface*, *121*, 2248–2269. https://doi.org/10.1002/2015JF003801

Bartholomaus, T. C., Anderson, R. S., & Anderson, S. P. (2008). Response of glacier basal motion to transient water storage. *Nature Geoscience*, *1*, 33–37. https://doi.org/10.1038/ngeo.2007.52

Bartholomaus, T. C., Anderson, R. S., & Anderson, S. P. (2011). Growth and collapse of the distributed subglacial hydrologic system of Kennicott Glacier, Alaska, USA, and its effects on basal motion. *Journal of Glaciology*, *57*(206), 985–1002. https://doi.org/10.3189/002214311798843269

Bartholomew, I. D., Nienow, P., Sole, A., Mair, D., Cowton, T., & King, M. A. (2012). Short-term variability in Greenland Ice Sheet motion forced by time-varying meltwater drainage: Implications for the relationship between subglacial drainage system behavior and ice velocity. *Journal of Geophysical Research*, *117*, F03002. https://doi.org/10.1029/2011JF002220

Bartholomew, I., Nienow, P., Mair, D., Hubbard, A., King, M. A., & Sole, A., et al. (2010). Seasonal evolution of subglacial drainage and acceleration in a Greenland outlet glacier. *Nature Geoscience*, *3*, 408–411. https://doi.org/10.1038/ngeo863

Bartholomew, I., Nienow, P., Sole, A., Mair, D., Cowton, T., Palmer, S., & Wadham, J. (2011). Supraglacial forcing of subglacial drainage in the ablation zone of the Greenland ice sheet. *Geophysical Research Letters*, *38*, L08502. https://doi.org/10.1029/2011GL047063

Bell, R. (2008). The role of subglacial water in ice-sheet mass balance. *Nature Geoscience*, *1*, 297–304. https://doi.org/10.1038/ngeo186

Bindschadler, R. (1983). The importance of pressurized subglacial water in separation and sliding at the glacier bed. *Journal of Glaciology*, *29*(101), 3–19. https://doi.org/10.3189/S0022143000005104

Carver, S., Sear, D., & Valentine, E. (1994). An observation of roll waves in a supraglacial meltwater channel, Harlech Gletscher, East Greenland. *Journal of Glaciology*, *40*(134), 75–78.

Chandler, D. M., Wadham, J. L., Lis, G. P., Cowton, T., Sole, A., Bartholomew, I., et al. (2013). Evolution of the subglacial drainage system beneath the Greenland Ice Sheet revealed by tracers. *Nature Geoscience*, *6*(3), 195–198. https://doi.org/10.1038/ngeo1737

Chen, G. (1998). *GPS kinematic positioning for airborne laser altimetry at Long Valley, California*. Cambridge, MA: Massachusetts Institute of Technology. Retrieved from http://dspace.mit.edu/handle/1721.1/9680

Christoffersen, P., Bougamont, M., Hubbard, A., Doyle, S. H., Grigsby, S., Pettersson, R. (2018), Cascading lake drainage on the Greenland Ice Sheet triggered by tensile shock and fracture. *Nature Communications 9*, 1064. https://doi.org/10.1038/s41467-018-03420-8

Chu, V. W. (2014). Greenland ice sheet hydrology: A review. *Progress in Physical Geography*, *38*(1), 19–54.

Chu, W., Schroeder, D. M., Seroussi, H., Creyts, T. T., Palmer, S. J., & Bell, R. E. (2016). Extensive winter subglacial water storage beneath the Greenland Ice Sheet. *Geophysical Research Letters*, *43*, 12484–12492. https://doi.org/10.1002/2016GL071538

Cooper, M. G., & Smith, L. C. (2019). Satellite remote sensing of the Greenland Ice Sheet Ablation Zone: A review. *Remote Sensing*, *11*, 2405. https://doi.org/10.3390/rs11202405

Cowton, T., Nienow, P., Sole, A., Bartholomew, I., & Mair, D. (2016). Variability in ice motion at a land-terminating Greenlandic outlet glacier: the role of channelized and distributed drainage systems. *Journal of Glaciology*, *62*(233), 451–466. https://doi.org/10.1017/jog.2016.36

Crozier, J., Karlstrom, L., & Yang, K. (2018). Basal control of supraglacial meltwater catchments on the Greenland Ice Sheet. *The Cryosphere*, *12*, 3383–3407. https://doi.org/10.5194/tc-12-3383-2018

Davison, B. J., Sole, A. J., Livingstone, S. J., Cowton, T. R., & Nienow, P. W. (2019). The influence of hydrology on the dynamics of land-terminating sectors of the Greenland ice sheet. *Frontiers of Earth Science*, *7*(10), 2296–6463. https://doi.org/10.3389/feart.2019.00010

Echelmeyer, K., & Harrison, W. D. (1990). Jakobshavns Isbræ, West Greenland: seasonal variations in velocity—Or lack thereof. *Journal of Glaciology*, *36*(122), 82–88.

Estey, L. H., and Meertens, C. M. (1999) TEQC: The multi-purpose toolkit for GPS/GLONASS Data. *GPS Solutions*, *3*(1), 42–49. https://doi.org/10.1007/PL00012778

Fausto, R. S., & van As, D. (2019). *Program for monitoring of the Greenland ice sheet (PROMICE): Automatic weather station data*. Version: v03, Dataset published via Geological Survey of Denmark and Greenland. Retrieved from https://doi.org/10.22008/promice/data/aws

Flowers, G. E. (2018). Hydrology and the future of the Greenland Ice Sheet. *Nature Communications*, *9*, 2729. https://doi.org/10.1038/s41467-018-05002-0

Flowers, G. E., Jarosch, A., Belliveau, P., & Fuhrman, L. (2016). Short-term velocity variations and sliding sensitivity of a slowly surging glacier. *Annals of Glaciology*, *57*(72), 71–83. https://doi.org/10.1017/aog.2016.7

Gagliardini, O., Cohen, D., & RåbackZwinger, P. T. (2007). Finite-element modeling of subglacial cavities and related friction law. *Journal of Geophysical Research*, *112*, F02027. https://doi.org/10.1029/2006JF000576

Gleason, C. J., Smith, L. C., Chu, V. W., Legleiter, C. J., Pitcher, L. H., Overstreet, B. T., et al. (2016). Characterizing supraglacial meltwater channel hydraulics on the Greenland Ice Sheet from in situ observations. *Earth Surface Processes and Landforms*, *41*, 2111–2122. https://doi.org/10.1002/esp.3977

Harper, J. T., Humphrey, N. F., Pfeffer, W. T., & Lazar, B. (2007). Two modes of accelerated glacier sliding related to water. *Geophysical Research Letters*, *34*, L12503. https://doi.org/10.1029/2007GL030233

Hoffman, M. J., Catania, G. A., Neumann, T. A., Andrews, L. C., & Rumrill, J. A. (2011). Links between acceleration, melting, and supraglacial lake drainage of the western Greenland Ice Sheet. *Journal of Geophysical Research*, *116*, F04035. https://doi.org/10.1029/2010JF001934

Holmes, G. (1955). Morphology and hydrology of the Mint Julep area, southwest Greenland. In *Project Mint Julep: Investigation of Smooth ice areas of the Greenland ice Cap, 1953; Part II: Special Scientific Reports*. Maxwell Air Force Base, AL: Arctic Desert Tropic Information Center, Research Studies Institute, Air University.

Howat, I. M., Tulaczyk, S., Waddington, E., & Björnsson, H. (2008). Dynamic controls on glacier basal motion inferred from surface ice motion. *Journal of Geophysical Research*, *113*, F03015. https://doi.org/10.1029/2007JF000925

IkenRöthlisberger, A. H., Flotron, A., & Haeberli, W. W. (1983). The uplift of Unteraargletscher at the beginning of the melt season — a consequence of water storage at the bed?. *Journal of Glaciology*, *29*(101), 28–47.

Irvine-Fynn, T. D. L., Hodson, A. J., Moorman, B. J., Vatne, G., & Hubbard, A. L. (2011), Polythermal glacier hydrology: A review, *Reviews of Geophysics*, *49*, RG4002. https://doi.org/10.1029/2010RG000350

Karlstrom, L., & Yang, K. (2016). Fluvial supraglacial landscape evolution on the Greenland Ice Sheet. *Geophysical Research Letters*, *43*, 2683–2692. https://doi.org/10.1002/2016GL067697

King, L., Hassan, M. A., Yang, K., & Flowers, G. (2016). Flow Routing for Delineating Supraglacial Meltwater Channel Networks. *Remote Sensing*, *8*(12), 988. https://doi.org/10.3390/rs8120988

Lampkin, D. J., & VanderBerg, J. (2014). Supraglacial melt channel networks in the Jakobshavn Isbræ region during the 2007 melt season. *Hydrological Processes*, *28*, 6038–6053. https://doi.org/10.1002/hyp.10085

McGrath, D., Colgan, W., Steffen, K., Lauffenburger, P., & Balog, J. (2011). Assessing the summer water budget of a moulin basin in the Sermeq Avannarleq ablation region, Greenland ice sheet. *Journal of Glaciology*, *57*(205), 954–964.

Meierbachtol, T., Harper, J., & Humphrey, N. (2013). Basal drainage system response to increasing surface melt on the Greenland Ice Sheet. *Science*, *341*(6147), 777–779. https://doi.org/10.1126/science.1235905

Nienow, P. W., Sole, A. J., Slater, D. A., & Cowton, T. R. (2017), Recent advances in our understanding of the role of meltwater in the Greenland Ice Sheet System. *Current Climate Change Reports*, *3*, 330–344, https://doi.org/10.1007/s40641-017-0083-9

Pitcher, L. H., & Smith, L. C. (2019). Supraglacial streams and rivers. *Annual Review of Earth and Planetary Sciences*, *47*(1), 421–452. https://doi.org/10.1146/annurev-earth-053018-060212

Pitcher, L. H., Smith, L. C., Gleason, C. J., Miege, C., Ryan, J. C., Hagedorn, B., et al. (2020). Direct observation of wintertime meltwater drainage from the Greenland Ice Sheet. *Geophysical Research Letters*, *47*, e2019GL086521. https://doi.org/10.1029/2019GL086521

Poinar, K., Joughin, I., Das, S. B., Behn, M. D., Lenaerts, J. T. M., & van den Broeke, M. R. (2015). Limits to future expansion of surface-melt-enhanced ice flow into the interior of western Greenland. *Geophysical Research Letters*, *42*, 1800–1807. https://doi.org/10.1002/2015GL063192

Price, S. F., Payne, A. J., Catania, G. A., & Neumann, T. A. (2008). Seasonal acceleration of inland ice via longitudinal coupling to marginal ice. *Journal of Glaciology*, *54*(185), 213–219. https://doi.org/10.3189/002214308784886117

Rennermalm, Å. K., Moustafa, S. E., Mioduszewski, J., Chu, V. W., Forster, R. R., Hagedorn, B., et al. (2013). Understanding Greenland ice sheet hydrology using an integrated multi-scale approach. *Environmental Research Letters*, *8*, 015017.

Rennermalm, Å. K., Smith, L. C., Chu, V. W., Box, J. E., Forster, R. R., & Van den Broeke, M. R. (2013), Evidence of meltwater retention within the Greenland ice sheet. *The Cryosphere*, *7*, 1433–1445, https://doi.org/10.5194/tc-7-1433-2013

Rennermalm, A. K., Smith, L. C., Hammann, A. C., Leidman, S. Z., Cooper, M. G., Cooley, S. W., & Pitcher, L. (2017). *River discharge at station AK-004-001, 2008-2016, version 3.0*. The State University of New Jersey, PANGAEA. https://doi.org/10.1594/PANGAEA.876357

Ryser, C., Lüthi, M. P., Andrews, L. C., Catania, G. A., Funk, M., Hawley, R. L., et al. (2014). Caterpillar-like ice motion in the ablation zone of the Greenland ice sheet. *Journal of Geophysical Research: Earth Surface*, *119*, 2258–2271. https://doi.org/10.1002/2013JF003067

Schoof, C. (2005). The effect of cavitation on glacier sliding. *Proceedings of the Royal Society A. 461*, 609–627. http://doi.org/10.1098/rspa.2004.1350

Smith, L. C., Chu, V. W., Yang, K., Gleason, C. J., Pitcher, L. H., Rennermalm, Å. K., et al. (2015). Efficient meltwater drainage through supraglacial streams and rivers on the southwest Greenland Ice Sheet. *Proceedings of the National Academy of Sciences of the United States of America*, *112*(4), 1001–1006. https://doi.org/10.1073/pnas.1413024112

Smith, L. C., Yang, K., Pitcher, L. H., Overstreet, B. T., Chu, V. W., Rennermalm, Å. K., et al. (2017). Direct measurements of meltwater runoff on the Greenland Ice Sheet surface. *Proceedings of the National Academy of Sciences of the United States of America*, *114*(50), E10622–E10631. https://doi.org/10.1073/pnas.1707743114

Stevens, L., Behn, M., McGuire, J., Das, S. B., Joughin, I., Herring, T., et al. (2015). Greenland supraglacial lake drainages triggered by hydrologically induced basal slip. *Nature*, *522*, 73–76. https://doi.org/10.1038/nature14480

Tedstone, A. J., Bartholomew, I., Chandler, D., Cowton, T., Mair, D., Nienow, P., & Sole, A. (2017). *Proglacial discharge measurements, Leverett Glacier, South-west Greenland (2009-2012)*. Natural Environment Research Council, Polar Data Centre. https://doi.org/10.5285/17c400f1-ed6d-4d5a-a51f-aad9ee61ce3d

Tedstone, A. J., Nienow, P. W., Sole, A. J., Mair, D. W. F., Cowton, T. R., Bartholomew, I. D., & King, M. A. (2013). Greenland ice sheet motion insensitive to exceptional meltwater forcing. *Proceedings of the National Academy of Sciences of the United States of America*, *110*(49), 19719–19724. https://doi.org/10.1073/pnas.1315843110

Tedstone, A., Nienow, P., Gourmelen, N., Dehecq, A., Goldberg, D., & Hanna, E. (2015). Decadal slowdown of a land-terminating sector of the Greenland Ice Sheet despite warming. *Nature*, *526*, 692–695. https://doi.org/10.1038/nature15722

van As, D., Bech Mikkelsen, A., Holtegaard Nielsen, M., Box, J. E., Claesson Liljedahl, L., Lindbäck, K., et al. (2017). Hypsometric amplification and routing moderation of Greenland ice sheet meltwater release. *The Cryosphere*, *11*, 1371–1386. https://doi.org/10.5194/tc-11-1371-2017

van As, D., Hasholt, B., Ahlstrøm, A. P., Box, J. E., Cappelen, J., Colgan, W., et al. (2019). *Program for monitoring of the Greenland ice sheet (PROMICE): Watson river discharge*. Version: v01, Dataset published via Geological Survey of Denmark and Greenland. Retrieved from https://doi.org/10.22008/promice/data/watson_river_discharge

van de Wal, R. S. W., Smeets, C. J. P. P., Boot, W., Stoffelen, M., van Kampen, R., Doyle, S. H., et al. (2015). Self-regulation of ice flow varies across the ablation area in south-west Greenland. *The Cryosphere*, *9*, 603–611. https://doi.org/10.5194/tc-9-603-2015

Williams, J. J., Gourmelen, N., & Nienow, P. (2020). Dynamic response of the Greenland ice sheet to recent cooling. *Scientific Reports*, *10*, 1647. https://doi.org/10.1038/s41598-020-58355-2

Yang, K., & Smith, L. C. (2013). Supraglacial streams on the Greenland Ice Sheet delineated from combined spectral-shape information in high-resolution satellite imagery. *IEEE Geoscience and Remote Sensing Letters*, *10*(4), 801–805. https://doi.org/10.1109/LGRS.2012.2224316

Yang, K., & Smith, L. C. (2016). Internally drained catchments dominate supraglacial hydrology of the southwest Greenland Ice Sheet. *Journal of Geophysical Research: Earth Surface*, *121*, 1891–1910. https://doi.org/10.1002/2016JF003927

Yang, K., Smith, L. C., Chu, V. W., Gleason, C. J., & Li, M. (2015). A caution on the use of surface digital elevation models to simulate supraglacial hydrology of the Greenland Ice Sheet. *IEEE Journal of Selected Topics in Applied Earth Observations and Remote Sensing*, *8*(11), 5212–5224. https://doi.org/10.1109/JSTARS.2015.2483483

Yang, K., Smith, L. C., Fettweis, X., Gleason, C. J., Lu, Y., & Li, M. (2019). Surface meltwater runoff on the Greenland ice sheet estimated from remotely sensed supraglacial lake infilling rate (2019). *Remote Sensing of Environment*, *234*, 111459. https://doi.org/10.1016/j.rse.2019.111459

Zwally, H. J., Abdalati, W., Herring, T., Larson, K., Saba, J., & Steffen, K. (2002). Surface melt induced acceleration of Greenland ice-sheet flow. *Science*, *297*(5579), 218222. https://doi.org/10.1126/science.1072708

Reference From the Supporting Information

Burkey, J. (2021). *Mann-Kendall Tau-b with Sen's method (enhanced).MATLAB Central File Exchange*. Retrieved from https://www.mathworks.com/matlabcentral/fileexchange/11190-mann-kendall-tau-b-with-sen-s-method-enhanced

Catania, G. A., & Neumann, T. A. (2010). Persistent englacial drainage features in the Greenland Ice Sheet. *Geophysical Research Letters*, *37*. L02501. https://doi.org/10.1029/2009gl041108. https://doi.org/10.1029/2009GL041108

Clason, C. C., Mair, D. W. F., Nienow, P. W., Bartholomew, I. D., Sole, A., Palmer, S., & Schwanghart, W. (2015). Modelling the transfer of supraglacial meltwater to the bed of Leverett Glacier, Southwest Greenland. *The Cryosphere*, *9*(1), 123–138. https://doi.org/10.5194/tc-9-123-2015. https://doi.org/10.5194/tc-9-123-2015

Cooper, M. G., Smith, L. C., Rennermalm, A. K., Miège, C., Pitcher, L. H., Ryan, J. C., et al. (2018). Meltwater storage in low-density near-surface bare ice in the Greenland ice sheet ablation zone. *The Cryosphere*, *12*(3), 955–970. https://doi.org/10.5194/tc-12-955-2018

Cowton, T., Nienow, P., Sole, A., Wadham, J., Lis, G., Bartholomew, I., et al. (2013). Evolution of drainage system morphology at a land-terminating Greenlandic outlet glacier. *J. Geophys. Res. Earth Surf.*, *118*, 29–41. https://doi.org/10.1029/2012jf002540. https://doi.org/10.1029/2012JF002540

Hoffman, M., Andrews, L., Price, S., Catania, G. A., Neumann, T. A., Lüthi, M. P., et al. (2016). Greenland subglacial drainage evolution regulated by weakly connected regions of the bed. *Nature Communications*, *7*. 13903. https://doi.org/10.1038/ncomms13903. https://doi.org/10.1038/ncomms13903

Jansson, P. (1996). Dynamics and hydrology of a small polythermal valley glacier. *Geografiska Annaler: Series A, Physical Geography*, *78*, 171–180. https://doi.org/10.1080/04353676.1996.11880463

Kamb, B. (1970). Sliding motion of glaciers: Theory and observation. *Rev. Geophys.*, *8*(4), 673–728. https://doi.org/10.1029/rg008i004p00673. https://doi.org/10.1029/RG008i004p00673

Lindbäck, K., Pettersson, R., Hubbard, A. L., Doyle, S. H., As, D., Mikkelsen, A. B., & Fitzpatrick, A. A. (2015). Subglacial water drainage, storage, and piracy beneath the Greenland Ice Sheet. *Geophys. Res. Lett.*, *42*, 7606–7614. https://doi.org/10.1002/2015gl065393. https://doi.org/10.1002/2015GL065393

Mair, D. W. F., Sharp, M. J., & Willis, I. C. (2002). Evidence for basal cavity opening from analysis of surface uplift during a high-velocity event: Haut Glacier d'Arolla, Switzerland. *J. Glaciol.*, *48*(161), 208–216. https://doi.org/10.3189/172756502781831502. https://doi.org/10.3189/172756502781831502

Morlighem, M., Williams, C. N., Rignot, E., An, L., Arndt, J. E., Bamber, J. L., et al. (2017). BedMachine v3: Complete bed topography and ocean bathymetry mapping of Greenland from multibeam echo sounding combined with mass conservation. *Geophysical Research Letters*, *44*, 11051–11061. https://doi.org/10.1002/2017gl074954. https://doi.org/10.1002/2017GL074954

Palmer, S., Shepherd, A., Nienow, P., & Joughin, I. (2011). Seasonal speedup of the Greenland ice sheet linked to routing of surface water. *Earth and Planetary Science Letters*, *302*(3–4), 423–428. https://doi.org/10.1016/j.epsl.2010.12.037

Ryan, J. C., Smith, L. C., van As, D., Cooley, S. W., Cooper, M. G., Pitcher, L. H., & Hubbard, A. (2019). Greenland Ice Sheet surface melt amplified by snowline migration and bare ice exposure. *Science Advances*, *5*(3). https://doi.org/10.1126/sciadv.aav3738. eaav3738. https://doi.org/10.1126/sciadv.aav3738

Schoof, C. (2010). Ice-sheet acceleration driven by melt supply variability. *Nature*, *468*(7325), 803. https://doi.org/10.1038/nature09618

Schweizer, J., & Iken, A. (1992). The role of bed separation and friction in sliding over an undeformable bed. *J. Glaciol.*, *38*(128), 77–92. https://doi.org/10.3189/s0022143000009618. https://doi.org/10.3189/S0022143000009618

Sugiyama, S., & Gudmundsson, G. H. (2004). Short-term variations in glacier flow controlled by subglacial water pressure at Lauteraargletscher, Bernese Alps, Switzerland. *J. Glaciol.*, *50*(170), 353–362. https://doi.org/10.3189/172756504781829846. https://doi.org/10.3189/172756504781829846

Shepherd, A., Hubbard, A., Nienow, P., King, M., McMillan, M., & Joughin, I. (2009). Greenland ice sheet motion coupled with daily melting in late summer. *Geophysical Research Letters*, *36*. L01501. https://doi.org/10.1029/2008gl035758. https://doi.org/10.1029/2008GL035758

Tedesco, M., Fettweis, X., Mote, T., Wahr, J., Alexander, P., Box, J. E., & Wouters, B. (2013). Evidence and analysis of 2012 Greenland records from spaceborne observations, a regional climate model and reanalysis data. *The Cryosphere*, *7*, 615–630. https://doi.org/10.5194/tc-7-615-2013. https://doi.org/10.5194/tc-7-615-2013

van As, D., Hasholt, B., Ahlstrøm, A. P., Box, J. E., Cappelen, J., Colgan, W., et al. (2018). Reconstructing Greenland Ice Sheet meltwater discharge through the Watson River (1949–2017). *Arctic Antarctic and Alpine Research*, *50*, 1. https://doi.org/10.1080/15230430.2018.1433799. https://doi.org/10.1080/15230430.2018.1433799

van de Wal, R. S. W., Boot, W., Van den Broeke, M. R., Smeets, C. J. P. P., Reijmer, C. H., Donker, J. J. A., & Oerlemans, J. (2008). Large and rapid melt-induced velocity changes in the ablation zone of the Greenland ice sheet. *Science*, *321*(5885). 111113. https://doi.org/10.1126/science.1158540

Yang, K., Smith, L. C., Karlstrom, L., Cooper, M. G., Tedesco, M., van As, D., et al. (2018). A new surface meltwater routing model for use on the Greenland Ice Sheet surface. *The Cryosphere*, *12*, 3791–3811. https://doi.org/10.5194/tc-12-3791-2018. https://doi.org/10.5194/tc-12-3791-2018

Yang, K., Sommers, A., Andrews, L. C., Smith, L. C., Lu, X., Fettweis, X., & Li, M. (2020). Inter-comparison of surface meltwater routing models for the Greenland Ice Sheet and influence on subglacial effective pressures. *The Cryosphere Discussions*. https://doi.org/10.5194/tc-2019-255